Acc. Chem. Res. **1998,** *31,* 717−725

Kinetic and Structural Analysis of Submillisecond Folding Events in Cytochrome *c*

M. C. RAMACHANDRA SHASTRY,[†]
J. MICHAEL SAUDER,[†,‡] AND
HEINRICH RODER*[,†,‡]

Institute for Cancer Research, Fox Chase Cancer Center, Philadelphia, Pennsylvania 19111, and Department of Biochemistry & Biophysics, University of Pennsylvania, Philadelphia, Pennsylvania 19104

Received April 20, 1998

Introduction

Much has been learned in recent years about the time scale and nature of elementary conformational changes in peptides and proteins.[1,2] While small proteins typically require milliseconds or longer to complete the process of folding, spectroscopic changes indicative of both local and long-range tertiary structural rearrangements are often found to occur on a much shorter time scale. However, the significance of these observations remains a topic of lively debate.[1,3−9] What determines the time scale of the first large-scale conformational events in folding? Is the condensation of the polypeptide chain driven by nonspecific hydrophobic interactions or by more specific tertiary interactions? Is the formation of compact states a gradual process governed by chain diffusion or a two-state transition limited by a discrete barrier in free energy?

The most commonly used approach for investigating the kinetics of protein folding relies on rapid mixing methods to initiate refolding via a sudden change in solvent conditions, coupled with optical detection (absorbance, fluorescence, circular dichroism, etc.) or hydrogen exchange labeling in conjunction with NMR. Although the time resolution of conventional stopped-flow and quenched-flow instruments is limited to a few milliseconds, one often finds that the observed kinetics does not account for the total change in the signal associated with the equilibrium unfolding transition, indicating that some conformational changes occur within the dead time of the measurement. This so-called burst-phase effect has been observed for numerous proteins, using various spectroscopic parameters, including circular dichroism (CD), intrinsic and extrinsic fluorescence probes, and protection of amide protons against solvent exchange (reviewed in refs 8 and 10−12). These observations are often attributed to the rapid accumulation of folding intermediates with some of the characteristics of a molten globule, i.e., a dynamic ensemble of compact states with high levels of secondary structure. On the other hand, it has also been suggested that the burst phase may simply reflect the initial response of the polypeptide chain to the change in solvent conditions, which favors formation of compact denatured states due to nonspecific hydrophobic interactions.[3,6,7]

Two possible folding scenarios are illustrated in Figure 1 in terms of simple kinetic schemes and the corresponding free energy diagrams expected under various conditions. Panel A depicts a minimal three-state mechanism where folding proceeds from the initial unfolded state, U, through an obligatory intermediate, I, to the native state, N (or a late folding intermediate). U represents the ensemble of unfolded conformations obtained immediately after the change in solvent conditions (which may contain clusters of nonrandom structure), whereas I represents an ensemble of partially folded states with distinct spectroscopic characteristics. The formation of I is described as a rapid (submillisecond) and reversible preequilibrium, U ⇌ I, which precedes the rate-limiting conversion of I into N. Under stabilizing conditions, I accumulates as a transient kinetic intermediate, giving rise to biphasic kinetics with a fast (often kinetically unresolved) transient followed by a slower phase observable on the stopped-flow time scale (>1 ms). Addition of denaturant lowers the free energies of partially and fully unfolded states relative to N, depending on the relative amounts of solvent-accessible surface area. Thus, the population of I decreases as we approach the unfolding transition region, and the slow phase gains amplitude at the expense of the fast phase, which is consistent with the observed burst-phase behavior. In Figure 1B, the polypeptide chain undergoes a rapid collapse from the initial extended conformation (D_1) into a more compact denatured conformation favored under stabilizing solvent conditions (D_i) before crossing the rate-limiting barrier (the various D-states are not necessarily sequential).

M. C. Ramachandra Shastry received his Ph.D. (1991) from the Indian Institute of Science, Bangalore, India, in solid state chemistry. After completing postdoctoral fellowships at the University of Bordeaux, the National Center of Biological Sciences, Bangalore, and the University of Mississippi, he joined the laboratory of Heinrich Roder in 1996, where he currently holds a Research Associate position. His research interests include kinetic and thermodynamic characterization of intermediates populated during early stages of protein folding.

J. Michael Sauder received his B. S. in chemistry from the University of Delaware (1991) and recently obtained his Ph.D. in structural biology and molecular biophysics from the University of Pennsylvania (1998), under the guidance of Heinrich Roder, using stopped-flow and quenched-flow techniques in the study of protein folding intermediates.

Heinrich Roder received his Ph.D. in biophysics from the Swiss Federal Institute of Technology (ETH Zürich) in 1981. Following postdoctoral work at the University of Illinois, he moved to the University of Pennsylvania, where he became Associate Professor in 1990 and Adjunct Professor in 1994. In 1991 he joined the Fox Chase Cancer Center as a Member of the Institute for Cancer Research and became a Senior Member in 1998. His research interests center around the mechanism of protein folding, protein structure, and protein dynamics. The approaches used by his group include NMR, hydrogen exchange, optical spectroscopy, and rapid mixing techniques.

* Correspondence should be addressed to this author at the Fox Chase Cancer Center. Phone: (215) 728-3123. Fax: (215) 728-3574. E-mail: H_Roder@fccc.edu.
[†] Fox Chase Cancer Center.
[‡] University of Pennsylvania.

10.1021/ar970086+ CCC: $15.00
Published on Web 10/22/1998

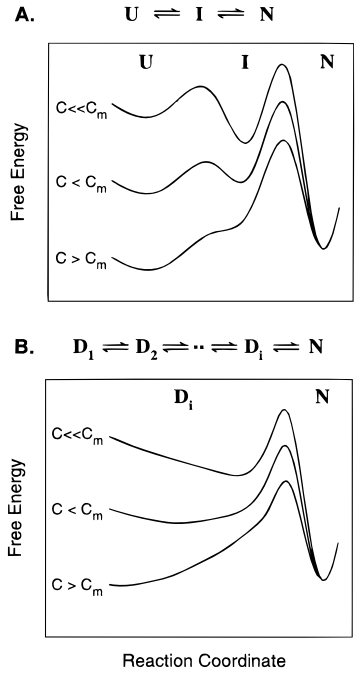

FIGURE 1. Schematic free energy diagrams expected for a three-state folding model (A) and a nonspecific collapse model (B) under strongly native (denaturant concentrations, C, far below the midpoint of the equilibrium unfolding transition, C_m), marginally stable ($C < C_m$), and denaturing ($C > C_m$) conditions.

Addition of denaturant results in a gradual shift from relatively compact to more extended denatured states. If the probe used to monitor the kinetics of folding is sensitive to chain compactness, such a random collapse model can also account for the observed burst-phase behavior. Although both models predict that the rate of the final folding step decreases with increasing denaturant concentration, accumulation of a discrete early intermediate can give rise to a pronounced kink ("roll-over") in a log rate vs [denaturant] plot (e.g., refs 13−16), which is not expected in the case of a continuous collapse.

The three-state model assumes that I is formed in a concerted two-state (first-order) transition, which predicts a sigmoidal dependence of the burst-phase amplitude on denaturant concentration. By contrast, a continuous (stepwise) collapse of the chain is likely to give rise to a more gradual denaturant dependence of the initial amplitude. A distinctly sigmoidal behavior indicative of well-populated intermediates has, in fact, been reported for several proteins.[17,18] However, the distinction is less clear-cut if intermediates are only marginally stable, as is often the case. The main feature that distinguishes the three-state model from the random collapse model is the presence of a well-defined barrier separating compact intermediates from the initial state, which predicts exponential kinetics for the formation of I from U. On the other hand, if the initial collapse of the chain is governed by diffusive dynamics, one expects nonexponential behavior.[19] To distinguish between the two models, it is, thus, essential to directly observe the conformational events during early stages of folding.

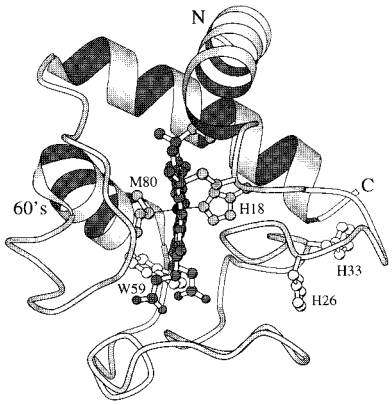

FIGURE 2. Ribbon diagram of horse cyt *c* (PDB 1HRC) showing the heme, the axial ligands His18 and Met80, potential nonnative ligands (His26 and His33), and Trp59, which serves as a fluorescence probe.

Rapid Mixing Methods

Several elegant methods have recently been introduced for initiating protein folding reactions more rapidly, using optical triggers[20,21] or temperature jumps.[22,23] These perturbation methods have provided intriguing insights into the dynamics of folding at early times, as described elsewhere in this issue. However, they are applicable only to certain proteins, and are often limited to conditions within or near the equilibrium unfolding transition where marginally stable folding intermediates are less likely to accumulate. In this respect, rapid mixing methods are more general and more versatile, especially since recent advances in mixer design and detection methods have made it possible to observe reactions in the submillisecond regime.[24−28] A particularly promising mixing method was introduced by Regenfuss et al.,[24] who showed that complete mixing of two solutions can be achieved within tens of microseconds by generating highly turbulent flow conditions in the wake of a small sphere placed at the junction of two concentric capillaries. We recently developed a continuous-flow mixing method that combines this mixer design with a sensitive charge-coupled device (CCD) detector, which makes it possible to obtain highly reproducible fluorescence measurements of reactions with time constants as short as 40 μs.[27] The sensitivity and resolution of the CCD detector allow us to acquire a complete reaction profile in a few seconds of continuous-flow operation consuming moderate amounts of reagents (fractions of a micromole of a protein containing a single tryptophan chromophore).

Kinetic Mechanism of Cytochrome *c* Folding

There are few proteins for which the folding mechanism has been investigated in as much detail as that of horse cytochrome *c* (cyt *c*). The presence of a covalently attached heme group in this 104-residue protein (Figure 2) serves as a useful optical marker, and its redox and ligand binding properties provide some unique experimental opportunities for exploring early stages of folding.[20,21,25] Its sole tryptophan residue, Trp59, is located

Scheme 1

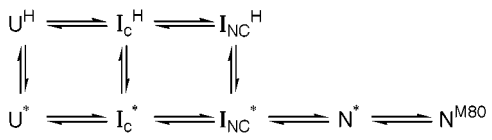

within 10 Å of the heme iron (Figure 2), resulting in efficient fluorescence quenching through a Förster-type energy transfer mechanism. Strongly denaturing conditions (e.g., 4.5 M guanidine HCl, or acidic pH at low ionic strength) result in a large increase in Trp59 fluorescence (up to ~60% of that of free tryptophan in water) indicative of an expanded chain conformation with an average tryptophan−heme distance greater than 35 Å.[26,29] Following extensive earlier studies,[30−34] we recently proposed a detailed kinetic mechanism (Scheme 1) that explains the complex folding and unfolding behavior of cyt *c* in terms of a tight coupling between structural transitions and heme ligand exchange events.[35]

The horizontal arrows represent major conformational transitions between fully unfolded states (U), early intermediates (I_c), late intermediates (I_{NC}), and nativelike states (N), whereas the vertical arrows indicate changes in heme ligation, as indicated by superscripts. Because of the adjacent Cys17−heme linkage, the native His18 ligand remains bound to the heme iron under typical denaturing conditions (e.g., 4.5 M guanidine HCl, pH > 3). However, the other native ligand, the sulfur of Met80, dissociates upon unfolding, resulting in a dynamic mixture of heme ligation states, which can give rise to multiple parallel folding pathways.[33] At acidic pH, the sixth iron coordination site remains vacant or binds a solvent molecule (U*),[36,37] whereas at higher pH (>6) it is occupied primarily by the deprotonated side chain of His33 (U^H).[38] The first structural intermediate in Scheme 1, I_c, can be described as an ensemble of relatively compact states containing loosely packed α-helices, on the basis of its partially quenched Trp59 fluorescence,[31,32] pronounced circular dichroism band at 220 nm,[32] protection of α-helical amide protons against solvent exchange,[39] and mutational analysis.[35] I_{NC} represents a subsequent intermediate that contains a subdomain of the native structure consisting of the close-packed N- and C-terminal helices, as evidenced by previous pulsed hydrogen exchange[31] and model peptide[40] studies. Kinetic analysis of mutant proteins with substitutions in the C-terminal helix confirmed that I_{NC} is stabilized by highly specific packing interactions of apolar side chains at the helix−helix interface.[35] In contrast, the stability of I_c involves less specific hydrophobic interactions, although the effect of truncating a key contact residue (mutation of Leu94 to Ala) suggests some preferential interaction between the terminal helices.

Because of its relatively slow rate of dissociation (~100 s^{-1}),[33] the nonnative histidine ligand remains bound during the initial stages of folding (in I_c^H and I_{NC}^H) and can get trapped during refolding. Misligation prevents proper folding in the middle segment of the chain (residues 20−89), but it does not interfere with the docking of the N- and C-terminal helices (Figure 2), resulting in accumulation of a partially folded intermediate (I_{NC}^H).[31] Dissociation of the nonnative His ligand ($I_{NC}^H \rightarrow I_{NC}$*) at a rate of about 10 s^{-1} represents the rate-limiting step for completing the folding process. If binding of a nonnative His ligand is prevented (e.g., by acidification or addition of an extraneous ligand, such as imidazole), the protein can bypass this slow step and proceed along a more direct path from U* to N^{M80}. The rate-limiting transition now occurs between I_c* and I_{NC}*, and the burst intermediate, I_c*, is the only partially folded state that accumulates to a significant level (at low denaturant concentrations).

Our kinetic mechanism (Scheme 1) is supported by a wealth of kinetic observations, including stopped-flow measurements of folding and unfolding monitored by fluorescence, heme absorbance, and CD over a wide range of conditions,[32−34,41] the kinetics of amide protection during folding,[31,33,34] as well as recent time-resolved resonance Raman measurements.[25,36] In fluorescence-monitored folding experiments, the formation of I_{NC}^H gives rise to a rapid phase on the 10 ms time scale, and the displacement of the nonnative His ligand by Met 80 produces a subsequent phase with a rate of about 10 s^{-1}. The trapping of nonnative histidine ligands can be avoided by protonating the imidazole group, or by addition of free imidazole to displace any intramolecular ligand at the sixth iron coordination site.[26,33,34] Pulsed hydrogen exchange and optically monitored folding experiments at pH 5 revealed a dominant folding process with a rate of about 80 s^{-1}, indicating that the misligated unfolded state (U^H) is no longer significantly populated.

Despite its complexity, Scheme 1 appears to be the simplest mechanism that can account for the bulk of experimental observations (excluding minor slow phases associated with species containing *cis*-prolyl peptide bonds). Although I_{NC}* is not directly observed, it is reasonable to assume that an intermediate resembling I_{NC}^H may also occur without trapping of a nonnative heme ligand. This assumption was confirmed by our recent observation that an intermediate with similar spectroscopic properties and response to mutations accumulates during folding at acidic pH (pH 2, high salt concentration), where a nonnative globular state (A-state) with the properties of a late folding intermediate is formed.[41] The presence of a nativelike species with only one axial heme ligand (N*) was revealed by unfolding experiments; the loss of the native methionine ligand can limit the rate of unfolding under strongly denaturing conditions (high denaturant concentrations or elevated temperature), where the rate of the N* → U* transition exceeds that of the N^{M80} → N* step.[17,35] N* does not accumulate to detectable levels under refolding conditions.

Direct Observation of Chain Collapse during Folding of Cyt *c*

The dramatic improvement in time resolution offered by our capillary mixing apparatus[27] enabled us to resolve the entire fluorescence-detected folding kinetics of cyt *c*,

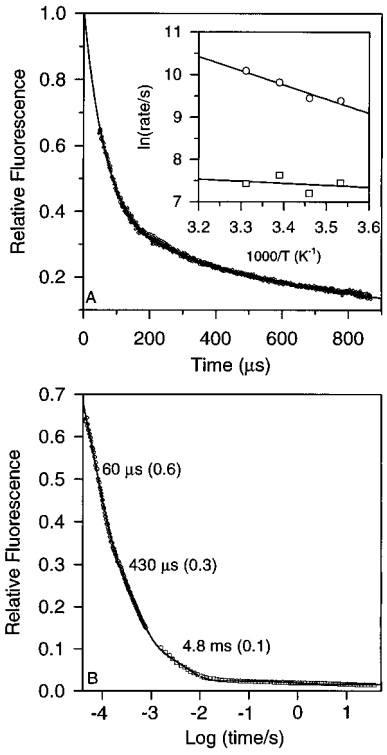

FIGURE 3. Refolding kinetics of acid-unfolded cyt *c* at pH 4.5, 22 °C.[42] (A) Submillisecond kinetics measured by continuous-flow mixing, indicating heme-induced quenching of Trp59 fluorescence associated with chain collapse. Inset: Arrhenius plot for the rates of the major (○) and the minor (□) submillisecond phases. (B) Combined plot of continuous-flow and stopped-flow kinetic traces measured under identical conditions. The time constants and relative amplitudes (in parentheses) are indicated for the three main phases.

including the elusive initial collapse of the chain.[42] As a representative example, Figure 3A shows the decay in Trp59 fluorescence observed during refolding of acid-unfolded cyt *c* (pH 2, 10 mM HCl) induced by a pH jump to native conditions (pH 4.5, 22 °C). The continuous-flow data covering the time range from 45 to 900 μs are accurately described by a biexponential decay with a major rapid phase (time constant 57 $\pm$ 5 μs) and a minor process in the 500 μs range. This fit extrapolates to an initial fluorescence of 1.0 $\pm$ 0.05 (relative to the acid-unfolded protein) at $t = 0$, indicating that no additional, more rapid fluorescence changes remain unresolved in the 45 μs dead time. The same data are plotted in Figure 3B on a logarithmic time scale, along with a stopped-flow trace measured under matching conditions, which accounts for the final 10% of the total fluorescence change. The combined kinetic trace covers 6 orders of magnitude in time and accounts for the complete change in Trp59 fluorescence associated with refolding of cyt *c*. An Arrhenius plot of the rate of the initial phase (Figure 3A, inset) yields an apparent activation enthalpy of 7.5 kcal/mol, which is somewhat larger than that expected for a diffusion-limited process,[43] but small compared to the activation enthalpy for unfolding of the native state (unpublished results).

In an extended series of continuous-flow experiments,[42] we measured the kinetics of folding of cyt *c* starting from either the acid-unfolded (pH 2, 10 mM HCl) or the GuHCl-unfolded state (4.5 M GuHCl, pH 4.5 or 7), and ending under various final conditions (pH 4.5 or 7 and GuHCl concentrations from 0.4 to 2.2 M). In each case, we observed a prominent initial decay in fluorescence with a time constant ranging from 25 to 65 μs. In particular, the rate of the initial phase, measured under the same final conditions (pH 4.5, 0.4 M GuHCl), was found to be independent of the initial state (acid- or GuHCl-unfolded). These observations clearly indicate that a common rate-limiting step is encountered during the initial stages of cyt *c* folding. The large amplitude of the initial phase (as much as 70% of the total change in fluorescence under strongly native conditions) is consistent with the formation of an ensemble of compact states, and the fact that the time course is exponential indicates that the rate of chain collapse is limited by a distinct free energy barrier, which separates the expanded initial conformations from compact states. The existence of such a barrier justifies the description of the initial folding events in terms of a model involving an early folding intermediate, as in Figure 1A. The first large-scale conformational event during folding of cyt *c* can thus be described as a reversible two-state transition. By contrast, these observations would be difficult to rationalize in terms of a nonspecific collapse (Figure 1B), since a gradual transition toward more compact states governed by diffusive dynamics is unlikely to give rise to exponential kinetics.[19] Although our results do not rule out the possibility of some contraction of the chain occurring concurrently with the change in solvent conditions, any conformational events preceding the 50 μs transition would have to be localized, since they do not give rise to any detectable quenching in Trp59 fluorescence. Our finding that the rate of collapse is insensitive to initial conditions suggests that the barrier may represent a general entropic bottleneck encountered during the compaction of the polypeptide chain, which is consistent with the moderate activation enthalpy associated with the initial transition (Figure 3A). Bryngelson et al.[19] classified this type of folding behavior as a "type I" scenario where a free energy barrier arises because of the unfavorable reduction in conformational entropy, which can be compensated by favorable enthalpic and solvent interactions only during the later stages of collapse.

Cytochrome *c* Folding and Heme Ligation

The coupling between heme ligation and conformational changes clearly plays an important role during the later stages of cyt *c* folding.[33,34,36] To test whether ligand rearrangements are also involved during the initial phases, we compared the kinetics of folding at pH 7 in the absence and presence of 0.2 M imidazole, which is known to block binding of any intramolecular ligands, whether native or nonnative, at the sixth iron coordination site.[26,33,44] Although these conditions lead to very different kinetic behavior at longer times, the rate of the major initial decay exhibits a time constant, $\tau = 65 \pm 5$ μs, irrespective of

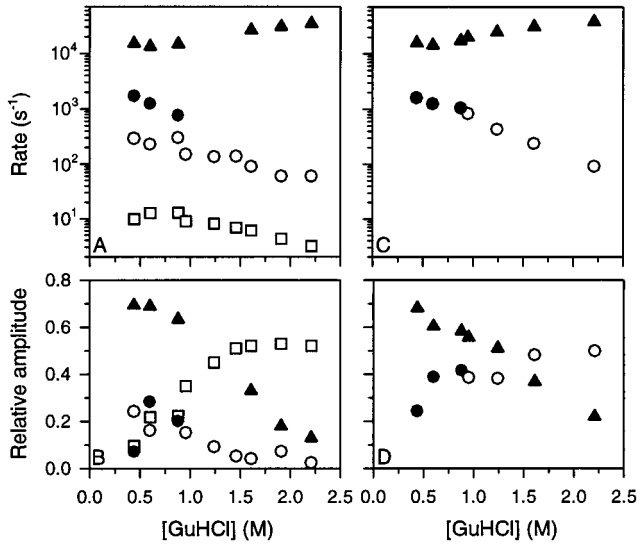

FIGURE 4. Refolding of GuHCl-unfolded cyt *c* at pH 7 (0.1 M phosphate, 22 °C) in the absence (A, B) and in the presence (C, D) of 0.2 M imidazole.[42] The GuHCl dependence of the rates (A, C) and amplitudes (B, D, using matching symbols) of refolding were measured by continuous-flow (filled symbols) and stopped-flow (open symbols) methods. An additional slow phase with a rate constant $<0.1\ s^{-1}$ and amplitude <15% observed under both conditions is omitted for clarity.

whether a nonnative histidine ligand or imidazole is bound to the heme iron. Thus, the formation of a compact intermediate is limited by an intrinsic conformational barrier rather than any rearrangements in heme ligation.

The rates and amplitudes obtained by fitting a series of exponentials to combined continuous-flow and stopped-flow traces are plotted in Figure 4 as a function of GuHCl concentration.[42] The kinetic behavior in the absence of imidazole (left-hand panels) is fully consistent with Scheme 1. In the unfolded state at neutral pH (U^H), the sixth iron coordination site is primarily occupied by His33.[38] The rapid formation of a compact intermediate with largely quenched Trp59 fluorescence, I_c^H, accounts for the 65 μs process, which dominates the kinetics at low GuHCl concentration (Figure 4B). The kinetic changes in the millisecond range (circles) are attributed to the formation of a second intermediate, I_{NC}^H, which was previously shown to contain tightly interacting N- and C-terminal α-helices, on the basis of pulsed hydrogen exchange[31] and mutagenesis[35] results. Although this intermediate contains a subdomain of the native structure, it maintains the nonnative His33−iron linkage, which blocks structure formation outside the N- and C-terminal segments.[33] The dissociation of the misligated histidine ($I_{NC}^H \rightarrow I_{NC}$*) gives rise to the rate-limiting process on the 100 ms time scale that becomes the major phase under destabilizing conditions (squares in panels A and B). The subsequent steps of folding, including formation of the native Met80−iron bond, occur rapidly without detectable intermediates (N* is observable only in unfolding experiments[17,35]). This mechanism (Scheme 1) is supported by the observation that the ligation-coupled slow step is greatly reduced in

Scheme 2

$$U^{Im} \rightleftharpoons I_c^{Im} \rightleftharpoons N^{Im}$$

amplitude at more acidic pH, where His33 is protonated and can no longer serve as a ligand.[33,34] The protein can then fold along a more direct path from U* to N^{M80} without encountering the slow ligand dissociation step. Our mechanism is further supported by a series of elegant studies by Rousseau and co-workers, who used resonance Raman spectroscopy for monitoring changes in heme ligation during folding of cyt *c*.[25,36] A unique feature of this approach is that it provides a direct measure of the concentrations of species with distinct axial ligands, although only those conformational changes that are coupled with ligation changes can be detected. The ligand exchange mechanism proposed by Yeh et al.[36] is related to Scheme 1, but does not distinguish some of the conformational states, such as I_c^H and I_{NC}^H, which are necessary to account for the fluorescence, CD, and hydrogen exchange labeling results.[31−33,42]

Even at pH 4.5 (the lowest value consistent with a stable native structure), there is evidence for some misligation, especially at elevated denaturant concentrations.[33,36] On the other hand, comparison of panels A and C of Figure 4 shows that the process in the 100 ms range is suppressed in the presence of imidazole, indicating that misligation can be avoided by binding of an extrinsic ligand. Despite this simplification, the folding kinetics of imidazole-bound cyt *c* exhibits two major phases with denaturant-dependent rates and amplitudes (Figure 4C,D), which cannot be explained by a two-state mechanism. Contrary to previous suggestions,[34,45] chain collapse is clearly not the rate-limiting step in folding, since its rate exceeds that of the final phase by an order of magnitude at low GuHCl concentrations and by a factor of 300 under destabilizing conditions (Figure 4C). The rate of the slower phase agrees well with recent fluorescence results obtained by Chan et al.[26] using a continuous-flow mixing apparatus with a dead time of about 80 μs. However, they were unable to resolve the faster process detected in our experiments, which has a time constant of 25−60 μs, depending on denaturant concentration. Our results for imidazole-bound cyt *c* can be modeled in terms of the minimal three-state mechanism shown in Scheme 2 where I_c^{Im} represents an ensemble of compact states analogous to I_c* in Scheme 1, and N^{Im} is the folded state under native conditions (an additional intermediate corresponding to I_{NC} may also be present, but does not accumulate to detectable levels in the presence of imidazole). In previous equilibrium studies, the imidazole complex of cyt *c* was shown to assume a stable nativelike conformation,[44,46] although the loss of the native Met80 sulfur−iron bond results in enhanced mobility.[47] Thus, N^{Im} can be considered a stable analogue of a late folding intermediate, or an early unfolding intermediate (corresponding to N* in Scheme 1).

The kinetic simplification due to imidazole binding made it possible to use quantitative kinetic analysis to

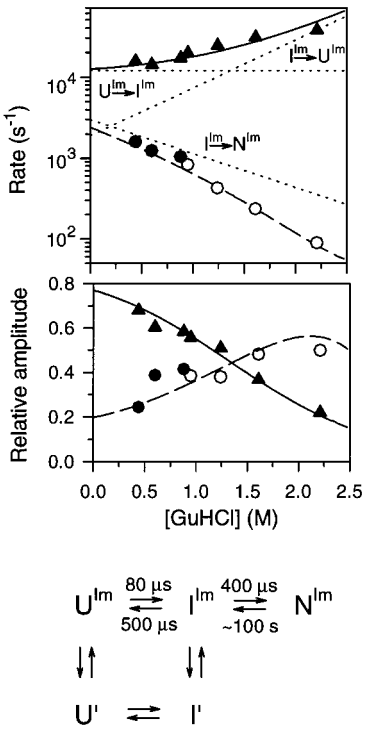

FIGURE 5. Kinetic folding mechanism of imidazole-bound cyt *c*.[42] The data are reproduced from Figure 4C,D. The lines represent the rates and amplitudes for the initial (solid) and final (dashed) folding phases predicted by the mechanism shown at the bottom. U′ and I′ represent a ~15% population of unfolded and collapsed states containing one or more nonnative (*cis*) proline peptide bonds, resulting in a minor slow phase (not shown). Dotted lines represent the microscopic rate constants vs guanidine HCl (GuHCl) concentration.

model folding as a function of denaturant concentration.[42] The observed rates and amplitudes are well described by the kinetics predicted on the basis of Scheme 2 (Figure 5). To account for a minor proline-related slow folding phase, a 15% population of unfolded molecules (U′) was assumed to fold along a parallel pathway via an intermediate, I′. As predicted in a previous study on ubiquitin,[16] addition of denaturant has little effect on the rate constant of the $U^{Im} \rightarrow I^{Im}$ transition, but accelerates unfolding of I^{Im} (dotted lines in Figure 5). The resulting depletion of I^{Im} accounts for the decrease in the observable rate of folding below that of the elementary $I^{Im} \rightarrow N^{Im}$ step. The model reproduces the observed dependence of the relative amplitudes on denaturant concentrations only if we assume that the intrinsic fluorescence yields of both I^{Im} and N^{Im} are close to zero. Thus, the measured amplitude of the initial phase reflects the denaturant-dependent population of compact states with largely quenched Trp59 fluorescence (as opposed to higher populations of partially quenched states). This analysis is consistent with I^{Im} being an obligatory intermediate. Although transient accumulation of an intermediate is expected to give rise to a lag in the appearance of the native state, this is experimentally observable only if the intermediate and the native state can be distinguished spectroscopically.[48,49]

Structural Properties of the Early Intermediate

The large decrease in fluorescence associated with the initial phase of cyt *c* folding (both in the presence and in the absence of a nonnative histidine−iron bond) is consistent with the transient formation of an ensemble of relatively compact states (I_c) in which the average distance between Trp59 and the heme is significantly shorter than 35 Å (the estimated Förster distance for energy transfer[26,50]). However, this does not necessarily imply that I_c is as compact as the native state, since efficient fluorescence quenching (>90%) is expected even for Trp59−iron distances up to ~24 Å. The early folding intermediate was previously found to be partially α-helical, on the basis of the observation that a substantial fraction of the native CD signal at 222 nm is recovered within a few milliseconds of refolding.[32] On the other hand, I_c appears to be highly dynamic, since earlier hydrogen exchange studies found no evidence for significant protection of amide protons against solvent exchange on the millisecond time scale.[31,33]

To gain more detailed insight into the structural properties of the early cyt *c* folding intermediate, we adopted a hydrogen exchange labeling protocol in which the labeling pulse is applied directly without a refolding delay.[51] As in the original competition experiment,[52] this burst-phase labeling method makes use of the competition between refolding and H/D exchange to probe structure formation during early stages of folding. This was achieved by rapidly mixing GuHCl-denatured cyt *c* in H_2O with a large excess of D_2O buffer at pD values in the range from 7.5 to 11.5.[39] Competition between refolding and H/D exchange was maintained for 2 ms before the pD was lowered to 5, where folding goes to completion in the absence of further exchange. The proton occupancies at 36 individual amide sites were then determined by two-dimensional NMR analysis.

Figure 6 summarizes the results[39] in terms of protection factors, *P*, which indicate the degree of protection against H/D exchange in the burst intermediate relative to a control experiment at higher denaturant concentration, where the intermediate is unstable. In contrast to the native state, where all of the amide protons analyzed are highly protected ($P = 10^3-10^8$),[53] many amide groups remain largely solvent-exposed ($P < 2$) in the early intermediate. However, a number of amide groups have acquired significant protection (3−8-fold) already within the first 2 ms of refolding. The highest protection factors observed are consistent with the stability of the early intermediate (0.9 ± 0.1 kcal/mol) determined by stopped-flow fluorescence measurements under the conditions of the competition experiment (pH 7−11). The ribbon diagram in Figure 6 shows that most of the well-protected residues (solid spheres) are found in the three main α-helices of the native structure. Such protection is not expected for isolated helical segments in the absence of stabilizing tertiary interactions, since N- and C-terminal peptide fragments of cyt *c* show low propensity (<20%) for α-helix formation.[40] A similar pattern, although with

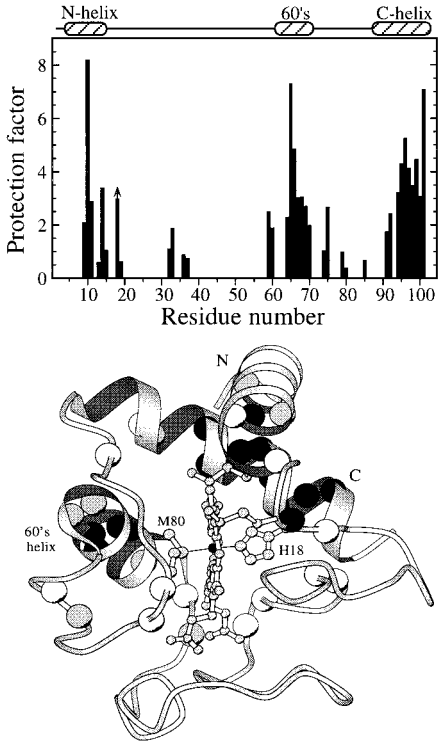

FIGURE 6. Protection of amide protons against H/D exchange within the first 2 ms of refolding of horse cyt *c* at variable pulse pH values (at 10 °C in D_2O, 0.3 M GuHCl, 0.4 M Na_2SO_4). Protection factors, *P*, for 36 amide protons, corrected for residual protection in the unfolded state, are plotted vs residue number.[39] Bottom: ribbon diagram of the native structure of horse cyt *c* showing the distribution of residues with well-protected (black, $P \geq 3$), partially protected (gray, $2 \leq P < 3$), and unprotected (white, $P < 2$) amide protons.

much higher protection factors (up to ~3000), has previously been observed in the equilibrium A-state of cytochrome *c*,[53] suggesting that both early and late folding intermediates are stabilized by a cluster of hydrophobically interacting α-helices. Thus, clear structural preferences are evident already during the initial stages of folding. By contrast, a nonspecific hydrophobic collapse is expected to give rise to lower protection factors and a more uniform distribution.

Summary and Conclusions

The continuous-flow mixing method recently developed in our laboratory,[27] which combines an efficient capillary mixer with a novel detection method employing a CCD camera, enabled us to monitor tryptophan fluorescence changes during refolding of cyt *c* down to tens of microseconds. In combination with conventional stopped-flow measurements, we were thus able to account for the entire time course of folding over 6 orders of magnitude in time, including the previously unresolved initial collapse of the polypeptide chain.[42] Our observation of a major exponential fluorescence decay with a time constant of about 50 μs indicates that the first large-scale conformational event in folding represents the barrier-limited formation of an ensemble of compact states. This free energy barrier has only a small enthalpic component, and its height varies little with initial and final refolding conditions, both in the presence and in the absence of nonnative heme ligands, indicating that it reflects a general entropic bottleneck encountered during the initial compaction of the polypeptide chain. In a recent hydrogen exchange labeling study,[39] we found that amide protons involved in α-helical hydrogen bonds of the native structure acquired weak but significant protection against solvent exchange within 2 ms of refolding, consistent with rapid formation of a core domain with loosely packed α-helices. This partially structured ensemble of states appears long before the rate-limiting folding step, even in the absence of slow extraneous steps, such as heme ligand exchange or peptide bond isomerization, indicating that folding occurs in at least two physically distinct stages. The results are fully consistent with a minimal three-state folding mechanism (Figure 1A) where a directed collapse of the chain into a loosely packed intermediate with some nativelike structural features precedes and facilitates the rate-limiting acquisition of the tightly packed native structure.

This research was supported by grants from the National Science Foundation (MCB-9306367) and the National Institutes of Health (GM56250).

References

(1) Eaton, W. A.; Muñoz, V.; Thompson, P. A.; Chan, C.-K.; Hofrichter, J. Submillisecond kinetics of protein folding. *Curr. Opin. Struct. Biol.* **1997**, *7*, 10−14.
(2) Callender, R. H.; Gilmanshin, R. Fast events in protein folding: The time evolution of primary processes. *Annu. Rev. Phys. Chem.*, in press.
(3) Fersht, A. R. Optimization of rates of protein folding: the nucleation-condensation mechanism and its implications. *Proc. Natl. Acad. Sci. U.S.A.* **1995**, *92*, 10869−10873.
(4) Baldwin, R. L. On-pathway versus off-pathway folding intermediates. *Folding Des.* **1996**, *1*, R1−R8.
(5) Wolynes, P. G.; Luthey-Schulten, Z.; Onuchic, J. N. Fast-folding experiments and the topography of protein folding energy landscapes. *Chem. Biol.* **1996**, *3*, 425−432.
(6) Creighton, T. E. How important is the molten globule for correct folding? *Trends Biochem. Sci.* **1997**, *22*, 6−11.
(7) Sosnick, T. R.; Shtilerman, M. D.; Mayne, L.; Englander, S. W. Ultrafast signals in protein folding and the polypeptide contracted state. *Proc. Natl. Acad. Sci. U.S.A.* **1997**, *94*, 8545−8550.
(8) Roder, H.; Colón, W. Kinetic role of early intermediates in protein folding. *Curr. Opin. Struct. Biol.* **1997**, *7*, 15−28.
(9) Clarke, A. R.; Waltho, J. P. Protein folding and intermediates. *Curr. Opin. Biotechnol.* **1997**, *8*, 400−410.
(10) Matthews, C. R. Pathways of protein folding. *Annu. Rev. Biochem.* **1993**, *62*, 653−683.
(11) Roder, H.; Elöve, G. A. In *Mechanisms of Protein Folding: Frontiers in Molecular Biology*; Pain, R. H., Ed.; Oxford University Press: New York, 1994; pp 26−55.

(12) Ptitsyn, O. B. Molten globule and protein folding. *Adv. Protein Chem*. **1995**, *47*, 83−229.
(13) Matouschek, A.; Kellis, J. T. J.; Serrano, L.; Bycroft, M.; Fersht, A. R. Transient folding intermediates characterized by protein engineering. *Nature* **1990**, *346*, 440−445.
(14) Parker, M. J.; Spencer, J.; Clarke, A. R. An integrated kinetic analysis of intermediates and transition states in protein folding reactions. *J. Mol. Biol.* **1995**, *253*, 771−786.
(15) Houry, W. A.; Rothwarf, D. M.; Scheraga, H. A. The nature of the initial step in the conformational folding of disulphide-intact ribonuclease A. *Nat. Struct. Biol.* **1995**, *2*, 495−503.
(16) Khorasanizadeh, S.; Peters, I. D.; Roder, H. Evidence for a three-state model of protein folding from kinetic analysis of ubiquitin variants with altered core residues. *Nat. Struct. Biol.* **1996**, *3*, 193−205.
(17) Sauder, J. M.; MacKenzie, N. E.; Roder, H. Kinetic mechanism of folding and unfolding of *Rhodobacter capsulatus* cytochrome c_2. *Biochemistry* **1996**, *35*, 16852−16862.
(18) Raschke, T. M.; Marqusee, S. The kinetic folding intermediate of ribonuclease H resembles the acid molten globule and partially unfolded molecules detected under native conditions. *Nat. Struct. Biol.* **1997**, *4*, 298−304.
(19) Bryngelson, J. D.; Onuchic, J. N.; Socci, N. D.; Wolynes, P. G. Funnels, pathways, and the energy landscape of protein folding: A synthesis. *Proteins* **1995**, *21*, 167−195.
(20) Jones, C. M.; Henry, E. R.; Hu, Y.; Chan, C.-K.; Luck, S. D.; Bhuyan, A.; Roder, H.; Hofrichter, J.; Eaton, W. A. Fast events in protein folding initiated by nanosecond laser photolysis. *Proc. Natl. Acad. Sci. U.S.A.* **1993**, *90*, 11860−11864.
(21) Pascher, T.; Chesick, J. P.; Winkler, J. R.; Gray, H. B. Protein folding triggered by electron transfer. *Science* **1996**, *271*, 1558−1560.
(22) Nölting, B.; Golbik, R.; Fersht, A. R. Submillisecond events in protein folding. *Proc. Natl. Acad. Sci. U.S.A.* **1995**, *92*, 10668−10672.
(23) Ballew, R. M.; Sabelko, J.; Gruebele, M. Direct observation of fast protein folding: the initial collapse of apomyoglobin. *Proc. Natl. Acad. Sci. U.S.A.* **1996**, *93*, 5759−5764.
(24) Regenfuss, P.; Clegg, R. M.; Fulwyler, M. J.; Barrantes, F. J.; Jovin, T. M. Mixing liquids in microseconds. *Rev. Sci. Instrum*. **1985**, *56*, 283−290.
(25) Takahashi, S.; Yeh, S.-R.; Das, T. K.; Chan, C.-K.; Gottfried, D. S.; Rousseau, D. L. Folding of cytochrome *c* initiated by submillisecond mixing. *Nat. Struct. Biol.* **1997**, *4*, 44−50.
(26) Chan, C.-K.; Hu, Y.; Takahashi, S.; Rousseau, D. L.; Eaton, W. A.; Hofrichter, J. Submillisecond protein folding kinetics studied by ultrarapid mixing. *Proc. Natl. Acad. Sci. U.S.A.* **1997**, *94*, 1779−1784.
(27) Shastry, M. C. R.; Luck, S. D.; Roder, H. A continuous-flow capillary mixer to monitor reactions on the microsecond time scale. *Biophys. J.* **1998**, *74*, 2714−2721.
(28) Bökenkamp, D.; Desai, A.; Yang, X.; Tai, Y.-C.; Marziuff, E. M.; Mayo, S. L. Microfabricated silicon mixers for submillisecond quench-flow analysis. *Anal. Chem*. **1998**, *70*, 232−236.
(29) Tsong, T. Y. The Trp-59 fluorescence of ferricytochrome *c* as a sensitive measure of the over-all protein conformation. *J. Biol. Chem*. **1974**, *249*, 1988−1990.
(30) Brems, D. N.; Stellwagen, E. Manipulation of the observed kinetic phases in the refolding of denatured ferricytochromes c. *J. Biol. Chem*. **1983**, *258*, 3655−3660.
(31) Roder, H.; Elöve, G. A.; Englander, S. W. Structural characterization of folding intermediates in cytochrome *c* by H-exchange labeling and proton NMR. *Nature* **1988**, *335*, 700−704.
(32) Elöve, G. A.; Chaffotte, A. F.; Roder, H.; Goldberg, M. E. Early steps in cytochrome *c* folding probed by time-resolved circular dichroism and fluorescence spectroscopy. *Biochemistry* **1992**, *31*, 6876−6883.
(33) Elöve, G. A.; Bhuyan, A. K.; Roder, H. Kinetic mechanism of cytochrome *c* folding: involvement of the heme and its ligands. *Biochemistry* **1994**, *33*, 6925−6935.
(34) Sosnick, T. R.; Mayne, L.; Hiller, R.; Englander, S. W. The barriers in protein folding. *Nat. Struct. Biol.* **1994**, *1*, 149−156.
(35) Colón, W.; Elöve, G. A.; Wakem, L. P.; Sherman, F.; Roder, H. Side chain packing of the N- and C-terminal helices plays a critical role in the kinetics of cytochrome *c* folding. *Biochemistry* **1996**, *35*, 5538−5549.
(36) Yeh, S.-R.; Takahashi, S.; Fan, B.; Rousseau, D. L. Ligand exchange during cytochrome *c* folding. *Nat. Struct. Biol.* **1997**, *4*, 51−56.
(37) Yeh, S.-R. Folding intermediates in cytochrome *c*. *Nat. Struct. Biol.* **1998**, *5*, 222−228.
(38) Colón, W.; Wakem, L. P.; Sherman, F.; Roder, H. Identification of the predominant non-native histidine ligand in unfolded cytochrome *c*. *Biochemistry* **1997**, *36*, 12535−12541.
(39) Sauder, J. M.; Roder, H. Amide protection in an early folding intermediate of cytochrome *c*. *Folding Des.* **1998**, *3*, 293−301.
(40) Wu, L.; Laub, P. B.; Elöve, G. A.; Carey, J.; Roder, H. A Noncovalent peptide complex as a model for an early folding intermediate of cytochrome *c*. *Biochemistry* **1993**, *32*, 10271−10276.
(41) Colón, W.; Roder, H. Kinetic intermediates in the formation of the cytochrome *c* molten globule. *Nat. Struct. Biol.* **1996**, *3*, 1019−1025.
(42) Shastry, M. C. R.; Roder, H. Evidence for barrier-limited protein folding kinetics on the microsecond time scale. *Nat. Struct. Biol.* **1998**, *5*, 385−392.
(43) Hagen, S. J.; Hofrichter, J.; Szabo, A.; Eaton, W. A. Diffusion-limited contact formation in unfolded cytochrome *c*: Estimating the maximum rate of protein folding. *Proc. Natl. Acad. Sci. U.S.A.* **1996**, *93*, 11615−11617.
(44) Babul, J.; Stellwagen, E. Participation of the protein ligands in the folding of cytochrome *c*. *Biochemistry* **1972**, *11*, 1195−1200.
(45) Sosnick, T. R.; Mayne, L.; Englander, S. W. Molecular collapse: the rate-limiting step in two-state cytochrome *c* folding. *Proteins* **1996**, *24*, 413−426.
(46) Shao, W.; Liu, G.; Tang, W. Binding of 1-methylimidazole to cytochrome *c*: Kinetic analysis and resonance assignments by 2D NMR. *Biochim. Biophys. Acta* **1995**, *1248*, 177−185.
(47) Roder, H.; Wand, A. J.; Milne, J. S.; Englander, S. W. Effect of methionine ligation on the structural dynamics of cytochrome *c* studied by 2D NMR observation of amide proton exchange. *Biophys. J.* **1986**, *49*, 57a.
(48) Walkenhorst, W. F.; Green, S. M.; Roder, H. Kinetic evidence for folding and unfolding intermediates in Staphylococcal nuclease. *Biochemistry* **1997**, *36*, 5795−5805.

(49) Heidary, D. K.; Gross, L. A.; Roy, M.; Jennings, P. A. Evidence for an obligatory intermediate in the folding of interleukin-1β. *Nat. Struct. Biol.* **1997**, *4*, 725−731.
(50) Jeng, M.-F.; Englander, S. W. Stable submolecular folding units in a noncompact form of cytochrome *c*. *J. Mol. Biol.* **1991**, *221*, 1045.
(51) Gladwin, S. T.; Evans, P. A. Structure of very early protein folding intermediates: new insights through a variant of hydrogen exchange labeling. *Folding Des.* **1996**, *1*, 407−417.
(52) Roder, H.; Wüthrich, K. Protein folding kinetics by combined use of rapid mixing techniques and NMR observation of individual amide protons. *Proteins* **1986**, *1*, 34−42.
(53) Jeng, M.-F.; Englander, S. W.; Elöve, G. A.; Wand, A. J.; Roder, H. Structural description of acid-denatured cytochrome *c* by hydrogen exchange and 2D NMR. *Biochemistry* **1990**, *29*, 10433−10437.

AR970086+